*Physical Review & Research International*
*4(1): 198-216, 2014*

**SCIENCEDOMAIN** *international*
www.sciencedomain.org

# Investigation of an Increase in Frequency of Scattered X-rays from a Silicon Single Crystal

**Biswajit Mallick**[1*]

[1]*Institute of Physics, Sachivalay Marg, Bhubaneswa 751005, India.*

***Author's contribution***

*The only author performed the whole research work. Author BM designed the study and wrote the first draft of the paper. Author BM read and approved the final version of the manuscript.*

***Research Article***

***Received 13th May 2013***
***Accepted 14th August 2013***
***Published 9th October 2013***

## ABSTRACT

**Aims:** X-ray scattered from a silicon single crystal was investigated. A new scattered line with increased frequency was observed.
**Study Design:** In order to ascertain that the new modified X-ray line observed is not accidental, an inelastic scattering experiment has been performed, using a grazing incidence X-ray instrument with a resolution of $2\times10^{-3}$.
**Place and Duration of Study:** Institute of Physics, Bubaneswar, India, between Jan 2011 and Nov 2011.
**Methodology:** In this experiment, X-rays are reflected from both the specimen and the focusing monochromator; which is known as reflection-reflection mode in double-crystal spectrometry (+1 -1). Incident radiation from an X-ray tube operated at 40 kV and 40 mA was used to obtain polychromatic CuK X-ray photons in the order of $10^{16}$ photon/s to observe a new scattering pattern from Compton effect caused excited plasmon (life time $10^{-16}$ s) standing wave in the silicon crystal.
**Results:** CuK X-rays scattered from silicon (333) crystal of 15 × 15 mm$^2$ and 1mm thick, possess unambiguous existence of a new modified line with increased frequency. The new scattering possesses high momentum transfer $k_p > k_c$, as high as $k_p$ = 6.16 ± 0.01 Å$^{-1}$ and ($k_p / k_F$)$^2$ = 8.9. These findings are in agreement with the previous plasmon scattering results reported by various authors. The total cross section of this scattering is experimentally found

[*]*Corresponding author: Email: bmallick_iopb@scientist.com;*

out to be 2.95 ± 0.009 × $10^{-22}$ $cm^2$/ electron and is inversely proportional to the third power of $k_p$. Both theoretically calculated and experimentally observed wavelength shift data match well with each other.

**Conclusion:** The new incoherent line was observed with the following major features: the energy of the new modified peak is greater than that of the Rayleigh peak; the new modified peak observed is narrower than the Compton peak for the same incident X-rays line.

*Keywords: X-ray scattering; compton effect; plasmon excitation; radiation interaction.*

## ABBREVIATIONS

*FFT Fast Fourier Transform*
*GIXRD grazing incidence X-ray diffraction*
*NR non-relativistic*
*NRI negative refractive index*
*RI refractive index*
*RPA random-phase approximation*

## 1. INTRODUCTION

Compton scattering is widely used as a unique and a very powerful tool for the investigation of electronic structure of materials of diverse nature [1-3]. Recent reports show that this effect covers various problems in advanced laser technology, accelerator-based radiation research and astrophysical studies [4-6], cancer therapy in medical physics [7-8]. Again, a number of good works on X-rays Compton effect caused plasmon scattering have already been reported by various authors [4-17]. In this radiation interaction (Compton effect) process, materials behave as a metamaterial because of plasmon excitation. In solid-state plasmas ($\varepsilon$<0, $\mu$>0), the square of the refractive index (RI), *i.e.*, $n^2$ becomes negative, which leads to reflection of X-ray waves from such a medium with higher frequency as in the case of inverse Doppler effect (radio waves) [18]. Substances with negative permittivity ($\varepsilon$) and permeability ($\mu$) have some properties which differ from those of substances with positive $\varepsilon$ and $\mu$. The critical density of plasmons can be defined as $n_c = (\varepsilon_0 m^* \omega_p^2)/e^2\ (1-\varepsilon\ ) = n_e/(1-\varepsilon)$, and RI of the plasmons has been defined as $n = \sqrt{1-(n_e/n_c)} = \pm R$, where $n_e$ is the electron density, $n_c$ is the critical plasmon density and $\varepsilon = \varepsilon_0 \in$ ($\in$ is the static dielectric constant and $\varepsilon_0 = 1/4\pi$ is a constant). The numerical factor of $R$ increases with a higher value of $\in$. From the above expressions related to $n_c$ and $\varepsilon$, the relation between electron density and static dielectric constant can be define qualitatively as $\frac{n_e}{n_c} + \varepsilon_0 \in = 1$. The electron density of silicon crystal $n_e$ ( $= \frac{Valency\ electron \times lattice\ point}{Volume\ of\ unit\ cell \times 10^{-24}\ cm^3}$) is $3\times10^{23}$. Again, the critical plasmon density $n_c$ is inversely proportional to the square of the X-ray wavelength ($\lambda$), *i.e.*, $n_c = \pi/(r_0\lambda^2)$, where $r_0$ (= $2.82\times10^{-13}$ cm ) is the "classical electron radius". X-rays of large $\lambda$ produce smaller value of $n_c$. It is clear from above relations that if $n_c$ decreases, RI becomes negative. So, for the negative refractive index (NRI), *i.e.*, $n = -R$, material behaves as a metamaterial [19]. Hence,

the dielectric constant of the above excited state can be simplified as $\in_d = 4\pi\left(n_c - n_e^{'}\right)/n_c$, where $n_e^{'}$ is the excited plasmon density. So far as the author's knowledge is concerned; there is no report on the scattered X-rays of increased frequency from materials like silicon. Therefore, the focus of this work is the physical origin of the enhancement in the frequency of the scattered X-rays.

In this paper, three novel results are presented: (1) theoretical model for the enhancement in the frequency of scattered wave, (2) derivation of the theory of impact between X-ray photon and Compton-effect-caused excited plasmon, and (3) experimental observation of the increase in X-ray energy using low-energetic photon from the single crystal silicon. In this experimental study, we have selected silicon as the scatterer because of three reasons: (a) Si-single crystals are the most perfect crystals with narrowest bandwidth available today, (b) silicon is commonly preferred for use as a pre-monochromator for relatively high-resolution work in X-ray spectroscopy, and (c) static dielectric constant of silicon crystal is quite impressive ($\in = 11.8$) as compared to other low-Z elements. Non-observance of this type of incoherent scattering peak in the earlier Compton scattering experiments may be due to the following reasons: (i) most of the earlier Compton scattering work was restricted to relatively hard radiation; (ii) intensity of incident X-rays drastically decreases upon use of a pre-monochromator at its initial stage; (iii) the new scattering was masked by Compton tail of the neighboring incident X-ray line; and (iv) the number of photons emitted per second was much less in X-ray sources used in earlier experiments. Thus, the observation of the X-ray effect (*i.e.*, incoherent scattering), which is presently under discussion, could have gone unnoticed.

The present work reports the theoretically predicted and experimentally observed new modified X-ray in single-crystal silicon. This new effect may be as useful as "Raman effect" and "Compton effect" for physicists and materials scientists to characterize materials of diverse nature. The new X-ray effect will give a new dimension to understand the electronic structure of materials in the same line as Compton effect.

## 2. THEORY

The quantum mechanical theory undoubtedly gives an adequate picture of the change in wavelength in Compton scattering. Applying Schrödinger and de Broglie hypothesis, the incident electron can be represented by a continuous train of $\psi$ waves of wavelength $\lambda_{matter} = h/(m_0 v/2)$, moving along the Y- direction (negative) and the recoil electron (atomic) by a similar wave train of the same wavelength moving along the Y-direction (positive), the two wave trains together will form standing waves (later referred as grating) for which the electronic charge density is proportional to $\psi_{inc}\psi_{rec}^{*}$ and the distance from the node to node is $(\lambda_{matter}/2) = h/(m_0 v)$. The de Broglie waves representing the electron thus form a Bragg grating space $d = h/(m_0 v)$ and will diffract the incident X-ray waves according to the usual expression $2d\sin\theta = \lambda$. The diffracted waves are modified in wavelength by the deflection because the grating is in motion (receding), resulting in a Doppler effect. For a wave (X-ray) traveling in normal dispersive media (stationary frame of reference) and incident on a receding grating, the receding grating velocity or group velocity ($v_{group}$) and the phase velocity ($v_{phase}$) of the incident wave (X-ray) are parallel; therefore, the incident field in the

frame of the receding grating oscillates with a relatively low frequency as expected for the conventional Doppler effect possessed Compton effect. In the anomalously dispersive medium (solid-state plasmon), the $v_{phase}$ of the incident wave and $v_{group}$ are anti-parallel. In this case, the incident field in the frame of approaching grating (in excited electron / plasma medium) oscillates with a relatively high frequency as expected for the inverse Doppler effect. Again RI is given as $n = c / v_{phase}$, which shows that for NRI material (solid-state plasma), the phase velocity becomes negative and $v_{group} = c^2 / (\pm v_{phase})$, so the approaching velocity. The experimental observation of the inverse Doppler effect, *i.e.*, increase of frequencies of reflected radiowaves from a receding boundary, has already been reported [16]. Hence, it is expected that X-rays reflected from the standing wave pattern approaching the solid-state plasma media, generated because of Compton effect, produce waves of increased frequency.

In Compton effect, a photon of energy $\hbar\omega_1$, after the collision scattered through an angle $2\theta$ from materials consisting of set of rest and free electrons having initial momentum $p_1$, becomes a scattered (Compton) photon of reduced energy $\hbar\omega_2$. These rest and free electrons absorb the amount of energy lost by the photon scattered with a momentum $p_2$. Hence, there is a vacancy in the atomic orbit. However, the number of positive charges in the centre remains constant. Then, the electron density fluctuation takes place. Hence, the excited oscillatory motion of fluctuating bound electrons possesses a new momentum $p_3$. These excited electrons, after transforming energy to another incident X-ray photon, attain a relaxed state of momentum $p_1'$, which is nearly the same as the initial momentum ( $p_1$ ). X-ray photon scattered from the above oscillating electrons (solid-state plasmon of energy $\hbar\omega_p$ ) shows a new type of incoherent scattering of enhanced energy $\hbar\omega_3$ . From energy-momentum conservation laws, we have

$$\hbar\omega_1 + \left(p_3^2/2m_0\right) = \hbar\omega_3 + \left(p_1'^2/2m_0\right) \tag{1}$$

or, $$p_3 = \hbar k_3 - \hbar k_1 + p_1 \qquad \left[\because p_1' = p_1\right] \tag{2}$$

where $p_3$ and $p_1$ are the initial and final momenta of excited plasmon, respectively. The $k_3$ ( $= \omega_3 / c$ ) is the final momentum of the new scattered photon and $\mathbf{k_p} = \mathbf{k_3} - \mathbf{k_1}$, is the scattering vector shown in Fig. 1. In the transition mechanism, the Compton scattering follows between lower ionization state (*i.e.*, intermediate state I) and bottom of the continuum state, and the new incoherent scattering follows between higher ionization state (*i.e.*, intermediate state II) and top of the continuum state.

Simplifying (Appendix-A), the energy of the newly scattered X-ray photon at an angle $2\theta'$ can be written as

$$\hbar\omega_3 = \frac{\hbar\,\omega_1}{\left[1-\gamma\left(1-\cos 2\theta'\right)\right]} - \frac{\left[2\,\hbar\omega_1\left(\frac{v'}{c}\right)\sqrt{\sin^2\theta'}\right]}{\left[1-\gamma\left(1-\cos 2\theta'\right)\right]} \tag{3}$$

This Eq. (3) is valid for all angles when $\gamma << 1$, *i.e*., non-relativistic photon (<15 keV). A non-relativistic (NR) description of incoherent scattering can be applied to X-ray below roughly 15 keV and in this energy range; the relativistic effect can be negligible. Again, in this incoherent X-ray scattering mechanism, the energy (momentum) transfer is very small (<1keV) compared to the $E_B$ (inverse of inter atomic distance $r_{nl}$ ) of the target system ( the collective scattering regime, $\Delta\hbar\omega << 1\ \mathrm{keV}$, $k\ r_{nl} << 1$ ).

As it is difficult to detect the scattered electron experimentally, one can only record the energy distribution of the scattered X-ray photons and then infer the momentum distribution of the electron. In order to extract the information regarding the momentum of the scattering electron, let us consider $q'$, the plasmon's initial state momentum and the new shift associated with the electron oscillation, which may be given as

$$\mathbf{q}' = \mathbf{k_p}\,.\,\mathbf{p}\ /\ \left|k_p\right| \tag{4}$$

where $k_p = \sqrt{(k_3 - k_1)^2} = \sqrt{k_3^2 + k_1^2 - 2k_1k_3\ \cos 2\theta'}$

Hence, $q'$ may be simplified as,

$$q' = \frac{(-137)\left\{\hbar\omega_3 - \hbar\omega_1 - \left(\hbar^2\omega_1\omega_3/m_0c^2\right)\left(1-\cos 2\theta'\right)\right\}}{\sqrt{\hbar^2\omega_1^2 + \hbar^2\omega_3^2 - 2\hbar^2\omega_1\omega_3\ \cos 2\theta'}} \tag{5}$$

where $m_0c = 137 = 1/\alpha$ and the $\alpha$ is the fine structure constant. Again, $m_0c\alpha = \hbar/a_0 = 1$ at. unit. (a.u.) of momentum (= 1.99275 × 10 $^{-19}$ g. cm/sec). In addition, 1a.u of energy is equal to 27.2 eV. For convenience, the electron momentum can be expressed in energy unit by multiplying it with the velocity of light '*c*'. So, 1 a.u of momentum (in energy unit) = 27.2 × 137.036 eV = 3.727 keV. Thus, with the help of the Eq. (5), the photon spectrum can be transformed to an electron (oscillatory) momentum spectrum.

The total cross section of this new incoherent scattering can be obtained by integrating the differential cross section over $\left(\frac{d\sigma}{d\Omega}\right)_N$ (Appendix-B), the solid angle, $d\Omega = 2\pi\ \sin\theta'\ d\theta'$.

$$\sigma_N = \int\left(\frac{d\sigma}{d\Omega}\right)_N d\Omega \tag{6}$$

Or, $$\sigma_N = \sigma_T\left(\frac{1}{k_p}\right)^3 M_c\,\frac{p_3}{p_2}\,(\in_d)^{\frac{1}{2}}\,n_e\int_0^{\pi} 2\pi\ \sin\theta'\ d\theta' \tag{7}$$

where $M_c$ ($\approx 2.756\times10^4$) is a constant quantity, since, $m_0c = 137$ and considering $\hbar = c = 1$, as used to study X-ray scattering from electron gas [20,21].

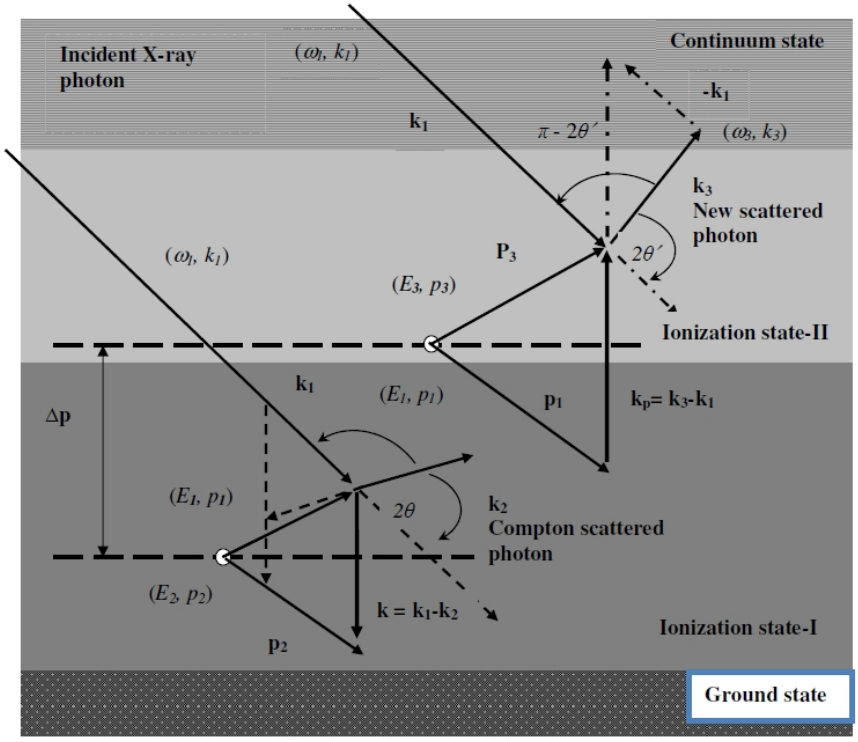


**Fig. 1. Schematic energy level diagram indicating the mechanism of: *(a)* Compton process in first intermediate ionization state (I, bound state) showing momentum conservation, where $p_1$ and $p_2$ are the initial and final momenta of the electron, $k_1$ and $k_2$, of the X-ray photon. $E_1$, and $E_2$, are the initial and final energies of the electron, $\omega_1$ and $\omega_2$, of the X-ray photon. The k is the scattering vector, which recedes from the collision centre; *(b)* new scattering process in the top of the second intermediate ionization state (II, bound state) showing momentum conservation, where $p_3$ and $p_1$ are the initial and final momenta (as assume in eq. (1), i.e., $p_1' = p_1$) of the excited electron (plasmon) due to Compton effect, $k_1$ and $k_3$ of the X-ray photon. $E_3$, and $E_1$, are the initial and final energies of the plasmon, $\omega_1$ and $\omega_3$, of the X-ray photon. The $\vec{k}_p$ is the scattering vector approaching the collision centre**

Finally, the total scattering cross section of this new scattering is found out to be

$$\sigma_N = \sigma_T \left(\frac{1}{k_p}\right)^3 (4\pi)^{\frac{3}{2}} M_c \frac{p_3}{p_2} \left( \left| \frac{n_c - n_e'}{n_c} \right| \right)^{\frac{1}{2}} n_e \qquad (8)$$

where the scattering vector $\mathbf{k_p}$ has magnitude $k_p = (4\pi/\lambda'')\sin\theta'$, which is a constant [22]. Again, the number of plasmons per unit volume $n_e'$ in a semiconductor, may be given by $n_e' = 4.8\times10^{21} T^{\frac{3}{2}} e^{-\Delta E/k_B T}$, where *T* is the temperature in degree Kelvin ($^\circ K$), and $k_B$ is the Boltzmann constant. In plasma physics, it is convenient to use the electron-volt as a unit of temperature ($^\circ K$) and is related as $1\,eV/k_B = 11604.505\,^\circ K$. Hence, the new scattering cross section is found out to be inversely proportional to the third power of momentum transfer, *i.e.*, $k_p^{-3}$. In addition, this new scattering cross section is found out to be directly proportional to the $\sqrt{\in_d}$ as predicted in the hypothesis. Also, the final momentum $p_3$ i.e., the momentum of the relaxed electron after scattering of the photon of enhanced energy, is the same as the initial momentum $p_1$, *i.e.*, $p_3 \approx p_1$. Since velocity ratio $\frac{v}{c} = \frac{1}{137.0377}\frac{Z}{n}$, where $Z = 14,$ and $n = 3$ (electron arrangement in the atom follows the $2n^2$ rule). Hence, the ratio of momenta $\frac{P_3}{P_1}$ or $\frac{v_3}{v_1}$ (velocity ratio) is calculated as 0.574.

## 3. EXPERIMENTAL DETAILS

The experimental setup consists of a grazing incidence X-ray diffraction (GIXRD) instrument, (Bruker AXS, D8 ADVANCE™ X-ray instrument) operated with monochramator in non-dispersive arrangement in parallel beam geometry with a resolution of $2\times10^{-3}$ used for the inelastic scattering study. The system shows the FWHM of 8.05 eV at 8 keV X-ray, which corresponds to a momentum resolution of about 0.05 a.u. A section through scattering geometry is shown in Fig. 2. The grazing-angle geometry is characterized by the deep penetration of X-rays into materials, hence the yield of inelastically scattered quanta drastically increases [20]. In this geometry, the sample was mounted in a two-axis goniometer; scanning was done by holding the angle of incidence constant (48.19°) and varying the diffraction angle $2\theta$ (= 96.34°) about the Bragg angle. Incident line focus $CuK_\alpha$ radiation from a high-power X-ray tube operated at 1600 W (40 kV and 40 mA) using a KRYSTALLO 780 X-ray generator. Again, source with the Be-window of the high-power tube having 95% transmissions emits $CuK_\alpha$ X-ray photons in the order of $1.2\times10^{16}$ photon/s (considering only 1% of power converted to polychromatic CuK X-ray). The $CuK_\alpha$ excitation from the line-focus tube, then the X-ray beam was collimated through fixed-divergence slit of 6 mm (≈ 3°) before irradiating the sample. The scattered X-ray beam from the sample was well collimated by passing through Soller slit of 0.23° before getting it reflected by LiF (100) crystal monochromator (d = 2.2265 Å). A NaI dynamic scintillation counter of quantum yield around 95% was mounted on the arm of the goniometer circle of radius 300 mm. Step size chosen for this experiment was 0.05° with scan rate of 0.05°/min (step). In this arrangement, X-rays are reflected from both the specimen and the focusing monochromator; which is known as reflection-reflection mode in double-crystal spectrometry (+1 -1) [2,21]. The observed spectral data were collected using a fully computer-controlled system and analyzed using software supplied by Bruker AXS, USA.

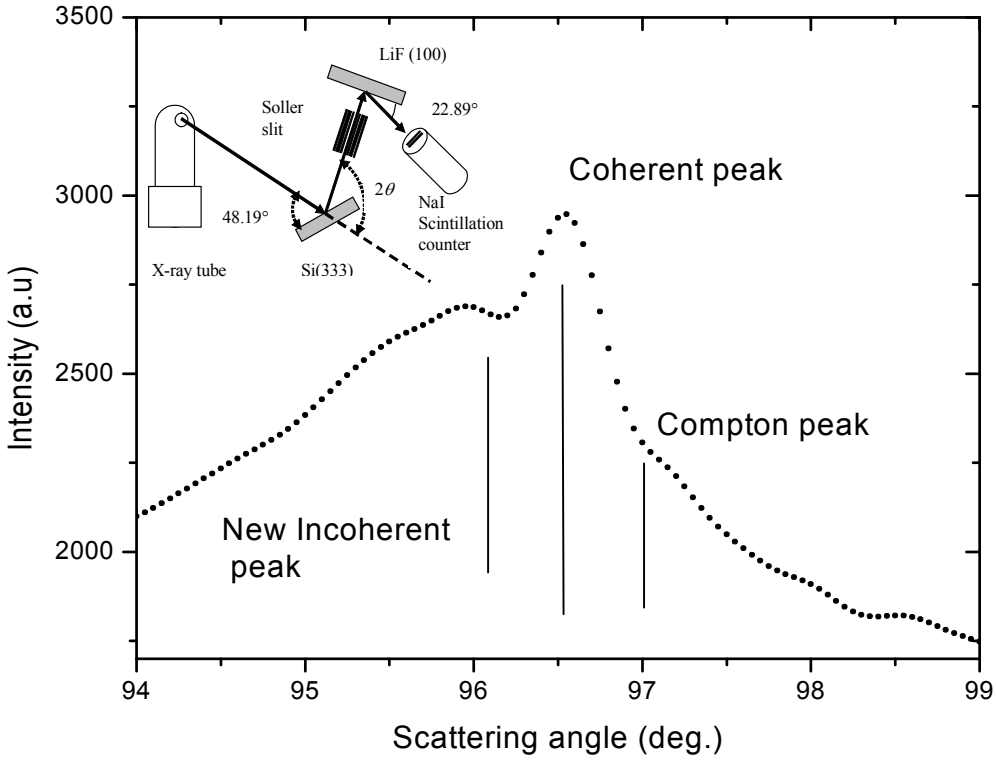


**Fig. 2. X-ray scattering spectra (accumulation of 10 hrs) of refined intensity data obtained from Si (333) crystal using CuK X-radiation incident at an angle 48.19°, applying GIXRD showing X-ray coherent peak, Compton scattered peak and a new incoherent scattering peak**

## 4. RESULTS AND DISCUSSION

Experimentally, it seems feasible to observe this kind of scattering phenomenon using low-energy X-ray photon. The lifetime of plasmon excitation and the incident photon flux are very sensitive and bear out the idea of the feasibility of this new type of scattering phenomena. The lifetime of the plasmon excitation [10,15] is of the order of $10^{-16}$ s, at the same time the lifecycle of the plasmon standing wave generated due to Compton effect (using low-energy X-rays of 10 keV), calculated using de Brogile's hypothesis, is of the order of $10^{-16}$ s. Since, the number of photons emitted by the source is of the order of $10^{16}$ photon/s, the possibility of this type of collision cannot be ignored. Hence, it is justified to think of the experimental feasibility of such type of X-ray scattering from the plasmon standing wave whose lifecycle is a few hundred times greater than the previous one (X-ray wave).

In order to ascertain that the new modified X-ray line observed is not accidental or a random one, experiments have been performed on different samples since 2000, using different X-ray wavelengths in both energy- and wavelength-dispersive spectrometers [22]. It was found that the existence of this new peak was as real and reproducible as the Compton peak and

was highly dependent upon scattering angle and characteristics of the scattering substances. Since then, various trials were taken to increase the intensity of this new scattering peak. In the present attempt, polychromatic ($CuK_{\alpha 1}$, $CuK_{\alpha 2}$, $CuK_{\beta}$, $CuL_{\alpha}$, etc.) X-rays were used instead of monochromatic X-rays for the Compton scattering experiment (post-monochromator was used instead of pre-monochromator). Comparing the intensity, the $CuK_{\alpha 2}$ and $CuK_{\beta}$ are, respectively, 0.5 and 0.2 times less intense than the $CuK_{\alpha 1}$. If perfectly monochromatic (using pre-monochromator) X-ray of the order of $10^{16}$ photons/sec is used, one can observe both Compton as well as this new effect. In such case, the Compton effect caused plasmon standing wave events are same as the amount of X-ray undergo Compton effect. However, in the second order interaction, i.e., X-ray interaction with plasmon standing wave is less probable (or nearly same) as compared to the Compton interaction. So, the new peak is less intense (or nearly same) as the Compton peak. Similarly, for polychromatic X-ray interaction with the crystal (sample), the amount of Compton effect caused plasmon standing wave events are more as compared to the earlier case. Using a post-monochromator set for $CuK_{\alpha 1,}$ one can observe Compton, Rayleigh peak of $CuK_{\alpha 1}$ and the new incoherent line respectively. In this case, interaction probability of $CuK_{\alpha 1}$ with plasmon standing wave produced due to multiple Compton effect ($CuK_{\alpha 1}$, $CuK_{\alpha 2}$, $CuK_{\beta}$, $CuL_{\alpha}$ , etc.) is more as compared to the earlier case. So the intensity of the new incoherent peak will be greater than or equal to the Compton peak. Again, the plasmon standing wave generated is directly proportional to the incident photon flux or the net incoming X-ray intensity, $I_0 (= I_{CuK\alpha 1}(1.0) + I_{CuK\alpha 2}(0.5) + I_{CuK\beta}(0.2) + ...)$. Hence, it is expected that the amount of standing wave generated using polychromatic CuK radiation can be increased around 1.7 times as compared to monochromatic $CuK_{\alpha 1}$. Again, at the recoil electron resonance condition (the Compton recoil electrons must build up standing waves in a direction normal to the lattice planes), the above intensity of the new scattered line will be highest due to the maximum interaction of standing wave with the X-ray photon. Because of this, relatively more intense peak as compared to Compton peak for the same material system was experimentally observed and is reported in the present paper. However, it is expected that this new peak intensity may decrease on increasing the scattering angle because of the damping of plasmons at higher scattering angle.

The scattered spectra of $CuK_{\alpha}$ (8.048 keV) X-rays by a 15 × 15 $mm^2$ and 1mm thick Si-single crystal using GXRD spectrometry was recorded. With an exposure of 10 hrs (40 kV and 40 mA), at an incident angle 48.19º, the spectra possess the usual coherent, incoherent (Compton) peaks and a new incoherent X-ray peak at low-angle side of the coherent peak ($CuK_{\alpha 1}$) was also observed. The total spectrum was collected with a scanning speed of 0.00083º/s. The profile fitting, smoothening (applying Adjacent Averaging, AA) and data refining (applying Fast Fourier Transform, FFT) were carried out using Origin 6.1 software. The 9-points AA-smoothened data with 5-points FFT-refined spectrum of the scattered spectra are shown in Fig. 2. The wavelength shift of the Compton peak, which varies with the scattering angle $2\theta$ (97.05º), was calculated to be about 0.0250Å (using the expression defined in Allison [21]. As stated, during Compton process the material target behaves as a metamaterial and the NRI of Si ($\in = 11.8$) was estimated to be -0.97. Because of NRI of the target material, X-rays of low frequency were scattered with high frequency. Wavelength shift in this process is found to be 0.0238Å experimentally for the Si (333), which matches well with the theoretically calculated value 0.0269Å and shown in Fig. 3. The intensity ratio (refined data) of the modified (Compton) to unmodified, *i.e.,* $I_c / I_r$ (=$R_c$) was found out to be 0.45. It is interesting to mention that a new peak of about 1.75 times more intensity than the Compton peak, as expected, was observed on the high-energy side (with respect to the

coherent peak) of the Si (333) spectra. The statistical counting error in the observed intensities of the new peak is about 0.05%. Intensity ratio of the above incoherent peak $I_a$ with usual unmodified peak $I_r$, *i.e.*, $I_a / I_r$ was found to be 0.78. The position of this new peak corresponded to an energy transfer of about 140 eV (high-energy side of the $CuK_{\alpha 1}$ line), whose Compton shift energy of about 142 eV (low-energy side of the $CuK_{\alpha 1}$ line). Experimentally, the width of the Compton profile (62 eV) was found out to be more than the new incoherent profile (43 eV). Hence, performing profile correction, the incoherently scattered photon energies $\hbar\omega_2$ and $\hbar\omega_3$ are found out to be 7.970 keV and 8.147 keV (Eq. (5)), respectively. Again, in impulse-approximation (IA) [23], $q \cong z$, the IA is valid over the range $-\infty$ to $+\infty$. The experimental data, however, can only be analyzed up to some finite upper limit on the long-wavelength side of the Compton profile $J(z)$. In actual practice, the solution to this problem is to select some convenient range from $-z$ to $+z$ that easily encompasses all the valance electron contribution, say 1.27 for silicon crystal [24]. In the present scattering study along Si (333), the profile functions $q$ (Compton) and $q'$ (new incoherent) were calculated for both types of scattering process and were found out to be + 0.719 a.u. and + 0.490 a.u., respectively. Again, this confirms that the energy exchange in the new process is lower as compared to the Compton process.

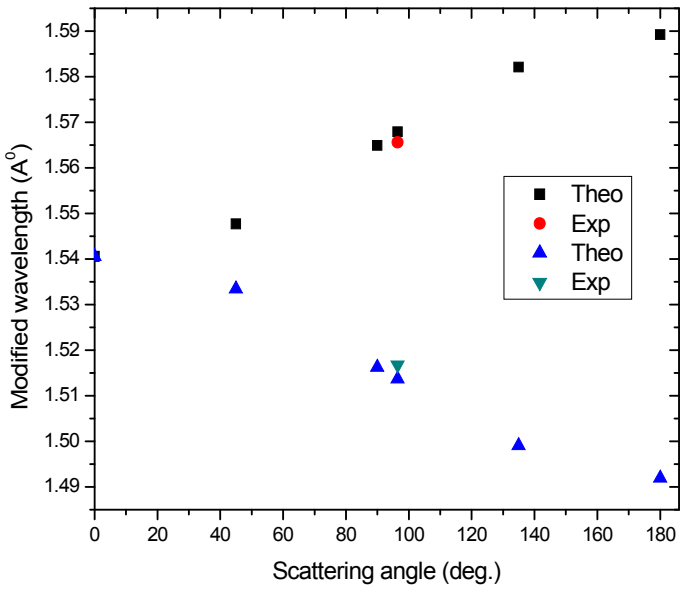


**Fig. 3. Modification of wavelength of $CuK_{\alpha 1}$ X-ray in Compton (■: theoretical,●: Experimental) and in new process (▲: theoretical , ▼: Experimental)**

According to random-phase approximation (RPA), X-ray scattering from plasmon appears clearly under the condition that $k$ is smaller than the critical wave vector $k_c$, *i.e.*, $k < k_c$. Though, the theoretical predictions for the dynamic structure factor of Si known so far are

restricted to the above range, and higher value of this RPA plasmon cut-off wave vector $k_c$ ( $=0.47\times\sqrt{r_s}\ k_F$ ) has been reported [25, 26], here $k_F(=\left[3\pi^2 n_e\right]^{\frac{1}{3}})$ is the Fermi wave vector and $r_s(=\left[47.11/\hbar\omega_p\right]^{\frac{2}{3}})$ is a dimensionless parameter [25]. As in the case of the dielectric of our interest, $\varepsilon(\omega,k)<0$ (where $\omega$ is real and $k$ is imaginary), the wave is damped with a characteristic length $1/|k_c|$ (plasmon cut-off vector), for silicon $k_c$ is around 1.38 Å$^{-1}$ [calculated with $n_e\cong 3\times10^{23}$ cm$^{-3}$, $\hbar\omega_p\approx16.6$ eV, $E_F\approx12.4$ eV and $k_F=2.07$ Å$^{-1}$]. The present experimental (Cuk X-ray scattering) results show high momentum transfer ( $k_p > k_c$), as high as $k_p$ = 6.16 ± 0.01 Å$^{-1}$ and ($k_p$ / $k_F$)$^2$ = 8.9, which is similar to the results reported in Suzuki and Tanokura [10], and Papademitriou and Miliotis [26] published separately, when CuK X-ray scattered from beryllium, ($k_p$ / $k_F$)$^2$ = 8.4 (where $k_c$ = 1.22 Å$^{-1}$). These results are in agreement with the previous finding [10,22,26]. This indicates that plasmons do not disperse when the momentum transfer exceeds the critical value. There is no exact theory available to define this high value of momentum transfer in plasmon scattering till date.

The wavelength-dependent critical electron density (theoretical critical density) $n_c\left(=\pi/(r_0\lambda^2)\right)$ in the present experiment is about $4.7\times10^{30}$ cm$^{-3}$. However, dielectric-constant dependent, $n_c\left(=n_e/1-\varepsilon_0\in\right)$ of silicon is $4.9\times10^{24}$ cm$^{-3}$ [calculated with $n_e\cong3\times10^{23}$ cm$^{-3}$, and $\in=11.8$]. Also, the excited plasmon density, $n_e'$ is found out to be $3.74\times10^{24}$ cm$^{-3}$ [calculated with $\Delta E=142$ eV, energy absorbed in Compton process]. The abrupt change of plasmon density at the crystal surface mainly depends on two factors: one is the temperature and the other one is the energy absorbed by the system and is defined in expression (8). In the present case, though the temperature of the system remains more or less constant, but the energy absorbed by the system $\Delta E$ , is large due to Compton effect. Because of this, the plasmon density increases exponentially ( $n_e'\propto T^{\frac{3}{2}}\ e^{-\Delta E/k_BT}$ ). Using the above $n_c$ and $n_e'$ values for silicon crystal, the $\in_d$ was calculated to be 2.98. A non-relativistic (NR) treatment can be applied to analyze the new scattering cross section. In Compton process, the total cross section for 10 keV X-rays is of the order of 10$^{-24}$ cm$^2$/electron. The total scattering cross section $\sigma_N$ , which is inversely proportional to the third power of the $k_p$ (equation (7)), is found to be 2.95 ± 0.009 ×10$^{-22}$ cm$^2$/electron. This is very close to the theoretically calculated result 2.88 ± 0.01 ×10$^{-22}$ cm$^2$/electron. However, the $\sigma_N$ is of the order of 10$^{-22}$ cm$^2$/electron, which indicates that the new cross section obtained is higher by two orders of magnitude as compared to the Compton cross section in NR region. The result is similar to the result obtained in electron Compton cross section, which is higher by five orders of magnitude [27]. Again, the $\sigma_N$ is directly proportional to $\sqrt{\in_d}$ as given in equation (7), which indicates that the materials of high value of dielectric constant

produce high value of $\sigma_N$. The instrument used for this purpose is sensitive (Compton effect) to the polarization of X-rays considering all the geometrical factors, where the polarization sensitivity of the device is a measure of asymmetry parameter A. However, asymmetry parameter of low-energy X-ray is given elsewhere [28]. Therefore, in the present X-ray instrument, the value of A is estimated to be 0.026 ± 0.002 ($CuK_\alpha$), using the theory suitable for the asymmetry of Thomson scattering spectrum (since Compton effect is less prominent in case of low-energy X-ray) [28].

Again, X-ray scattering from plasmon with $k > k_c$ has also been experimentally observed [14,16,29,30]. This large value of the damping constant may be because of quadratic dispersion of RPA Lindhard-type dielectric constant [31]. In addition, the plasmon dispersion curve bent over for larger values of *k* and showed little dependence of $\omega$ and *k*. The calculated bandwidth [32,33], $W_B$, of the analyzing crystal (post-monochromator) can be expressed as $\frac{\Delta\lambda}{\lambda}$, where $\Delta\lambda$ is the product of the receiving slit width $w_R$ (same as Soller slit for the present setup) and the reciprocal of the linear dispersion, $\frac{d\theta}{d\lambda}$ $\left(=\frac{\tan\theta}{\lambda}\right)$. So, the $W_B\left(=\frac{w_R}{\tan\theta}\frac{\lambda}{\lambda}\frac{1}{\lambda}=\frac{0.23°}{\tan 48.19°}\right)$ is 0.21º. However, the total separation is around 0.42º, since the diffractometer always read $2\theta$. Based on the above bandwidth calculation, there was no extra diffraction peak identified. Weak and extended diffuse scattering peak from the epitaxial Si layer in the X-ray rocking curve around the Si(333)-substrate reported by Fenske et al. [34] supports the above finding.

## 5. CONCLUSION

In the present paper, theoretically predicted and experimentally observed new modified X-ray peak in single-crystal silicon using polychromatic X-ray has been reported. The new incoherent line was observed to have the following major features: (i) the energy of the new modified peak is greater than that of the Compton peak; (ii) the new modified peak observed is more intense and narrower compared to the Compton peak for the same incident X-ray line; and (iii) the new modified peak observed is better resolved than the Compton peak for the same scattering angle. Since the broadening of scattering peak decreases with increasing incident energy and vice-versa, so the Compton peak is not cleared in case of low energy X-rays. Thus, the non-observance of this type of incoherent scattering peak in earlier experiments is probably due to the absence of polychromatic quantum interaction mechanism. Although our use of relatively low-intensity X-ray source, is unable to provide precise data, it is expected that, use of more intense X-ray source (e.g., 3$^{rd}$ generation synchrotron radiation or Free electron laser), X-ray detectors of excellent energy resolution, advanced Compton spectrometer, suitable scattering angles and materials (possessing low atomic number, high dielectric constant) will, no doubt, provide a more prominent new modified peak with better signal-to-noise ratio. Such a scenario is likely to provide better understanding of the electron density distribution of solids. Also, it is expected that this new effect will give a new dimension to understand the electron dynamics and electronic structure of materials.

## ACKNOWLEDGEMENTS

The author would like to express his thanks to Professor S. N. Sahu and Dr. S. N. Sarangi of the Institute of Physics, Bhubaneswar, India, for their assistance in performing the experiment. In addition, the author is indebted to Professor T. N. Tiwari, unique Research Centre, Rourkela, and Professor B. K. Das, Gauhati University, Gauahati, India for reading and spending their valuable time to correct the contents of manuscript.

## COMPETING INTERESTS

Author has declared that no competing interests exist.

## REFERENCES

1. Compton AH. A Quantum theory of the scattering of X-rays by light elements. Phys. Rev. 1923;21(5):483-502.
2. Compton AH, Allison SK. X-ray in Theory and Experiment. New York: D Van Nostrand Company Inc; 1960.
3. Williams B, editor. Compton Scattering. Great Britain: McGraw-Hill; 1977.
4. Piazza AD, Hatsagortsyan KZ, Heitel CH. Quantum Radiation Reaction Effects in Multiphoton Compton Scattering. Phys. Rev. Lett. 2010;105:220403-1-220403-4. DOI: 10.1103/PhysRevLett.105.220403.
5. Hartemann FV, Albert F, Siders CW, Barty CPJ. Low-Intensity Nonlinear Spectral Effects in Compton Scattering. Phys. Rev. Lett. 2010;105:130801-1-130801-4. DOI: 10.1103/PhysRevLett.105.130801.
6. Bocquet JP, Moricciani D, Bellini V, Beretta M, Casano L, D'Angelo A, et al. Limits on Light-Speed Anisotropies from Compton Scattering of High-Energy Electrons. Phys. Rev. Lett. 2010; 104: 241601-1-241601-5. DOI:10.1103/PhysRevLett.104.241601.
7. Spies L, Evans PM, Partridge M, Hansen VN, and Bortfied T. Direct measurement and analytical modeling of scatter in portal imaging. Med. Phys. 2000;27(3):462-471.
8. Spies L, Bortfied T. Analytical scatter kernels for portal imaging at 6 MV. Med. Phys. 2001;28(4):553-559.
9. Priftis G, Plasmon Excitation in Compton-Scattering Experiments. Phys. Rev. B. 1970;2:54-59. DOI:10.1103/PhysRevB.2.54.
10. Suzuki T, Tanokura A. X-Ray Plasmon Scattering. I. Experiment on Beryllium. J. Phys. Soc. Jpn. 1970;29:972-978. DOI: 10.1143/JPSJ.29.972.
11. Dubois DF, Gilinsky V. Incoherent Scattering of Radiation by Plasmas. I. Quantum Mechanical Calculation of Scattering Cross Sections. Phys. Rev. 1964;133:A1308-A1317. DOI:10.1103/PhysRev.133.A1308.
12. Ohmura Y, Matsudaira N. Influence of Coulomb Correlation on the Scattering of X-Ray by an Electron Gas. I. RPA Approximation. Phys. Soc. Jpn. 1964;19:1355-1360. DOI: 10.1143/JPSJ.19.1355.
13. Platzman PM. Incoherent Scattering of Light from Anisotropic Degenerate Plasmas. Phys. Rev. 1965;139: A379-A387. DOI:10.1103/PhysRev.139.A379. and, Resonant Compton scattering. Phys. Rev. B. 1989;40;5883-5885. DOI:10.1103/PhysRevB.40.5883.
14. Platzman PM, Tzoar N. X-Ray Scattering from an Electron Gas. Phys. Rev. 1965;139:A410-A413. DOI: 10.1103/PhysRev.139.A410.
15. Miliotis DM. Bulk-Plasmon Dispersion Spectrum of Be Using an X-Ray Scattering Technique. Phys. Rev. B. 1971;3:701-705. DOI: 10.1103/PhysRevB.3.701.

16. Alexandropulos NG. X-Ray Plasmon Scattering of Lithium. J. Phys. Soc. Jpn. 1971;31:1790-1795. DOI: 10.1143/JPSJ.31.1790.
17. Eisenberger P, Platzman PM, Pandy KC. Investigation of X-Ray Plasmon Scattering in Single-Crystal Beryllium. Phy. Rev. Lett. 1973;31;311-314. DOI: 10.1103/PhysRevLett.31.311.
18. Seddon N**,** Bearpark T. Observation of the Inverse Doppler Effect**.** Science. 2003;302**:**1537**-**1540. DOI: 10.1126/science.1089342.
19. Padilla WJ, Basov DN, Smith DR. Negative refractive index metamaterials, Mater. Today. 2006;9(7-8):28-35.
20. Afanasev AM, Imamov RM, Mukhamedzhanov EK, Nazlukhanyan AA. Coherent Compton Effect in the Grazing Bragg-Laue Geometry. Phys. Stat. Sol. A 1987;104(2):K73-K77. DOI: 10.1002/pssa.2211040249.
21. Allison SK. On the Generalization of the Notation for the Double Crystal X-Ray Spectrometer. Phys. Rev. 1937;52(8): 884-885. DOI: 10.1103/PhysRev.52.884.
22. Mallick B. New X-ray Scattering from Polymers and its Quantum Profile Analysis Applied to Materials Characterisation. SPIE Conf. Proc. 2001;4329:311-318. and, A Quantum theory of the scattering of soft X-ray from Compton effect caused electron standing wave in the materials. Turk. J. Phys. 2011;35(2):75-114.
23. Currat R, DeCicco PD, Weiss RJ. Impulse Approximation in Compton Scattering. Phys. Rev. B 1971;4(12):4256-4261. DOI:10.1103/PhysRevB.4.4256.
24. Bushuev VA, Kazimirov AY, Koval'chuk MV. Determination of the valence-electron component of the atomic scattering factor of silicon by means of a Compton effect excited by an x-ray standing wave. JETP Lett. 1988;47:187-191.
25. Srivastava KS. Influence of electron exchange energy on X-ray plasmon scattering by solids. Solid State Commun. 1979;30(1):19-20.
26. Papademitriou D, Miliotis D. Bonding-antibonding and plasmon bands of the Cu-Kβ X-ray spectrum from a polycrystalline beryllium scatterer. Solid State Commun. 1983;48:799-801.
27. Schattschneider P, Exner A. Progress in Electron-Compton scatering. Ultramicroscopy. 1995;59:241-253.
28. Wrubel T, Glenzer S, Buscher S, Kunze HJ. Investigation of electron-proton drifts with Thomson scattering. J. Atmos. Terre. Phys. 1996;58:1077-1087.
29. Kliewer KL, Raether H. Plasmon Observation Using X- Rays. Phys. Rev. Lett. 1973;30(20):971-974. DOI:10.1103/PhysRevLett.30.971.
30. Schülke W, Schmitz JR, Schulte-Schrepping H, Kaprolat A.Dynamic and static structure factor of electrons in Si: Inelastic X-ray scattering results. Phys. Rev. B 1995;52(16):11721-11732. DOI:10.1103/PhysRevB.52.11721.
31. Höhberger HJ, Otto A, Petri E. Plasmon resonance in Al, deviations from quadratic dispersion observed. Solid State Commun. 1975;16(1):175-179.
32. Itou M, Harada T, Kita T. Soft x-ray monochromator with a varied-space plane grating for synchrotron radiation: design and evaluation. Appl. Opts. 1989;28(1):146-153.
33. Cooper MJ. Compton scattering and electron momentum determination. Rep. Prog. Phys. 1985;48(4):415-481. doi:10.1088/0034-4885/48/4/001.
34. Fenske F, Schulze S, Hietschold M, Schmidbauer M. Structural investigations of homoepitaxial Si films grown at low temperature by pulsed magnetron sputtering on Si(111) substrates. Thin Solid Film. 2008;516(2):4777-4783.

## APPENDIX-A

The amount of energy transferred to X-ray photon from plasmon may be written applying Eqn. (1) and Eqn. (2) as

$$\Delta\omega\big|_N = \omega_3 - \omega_1 = \left(p_3^2/2m_0\right) - \left(p_1^2/2m_0\right)$$
$$= \left(p_1 + k_p\right)^2/2m_0 - \left(p_1^2/2m_0\right)$$

So, $$\Delta\omega\big|_N = \left(k_p + p_1\right)^2/2m_0 - \left(p_1^2/2m_0\right)$$

Or, $$\Delta\omega\big|_N = \left(k_p^2/2m_0\right) + \left(k_p.p_1/m_0\right) \quad \text{(A1)}$$

Now, the Eqn. (A1) contains an extra term, which is also linearly dependent on the electrons ground state momentum and the inverse Doppler shift associated with electron in plasmon excitation. Hence, the new profile of the scattered photon is centered on $k_p^2/2m_0$ with a width $\mathbf{k_p}.\mathbf{p_1}/m_0$.

Here $\mathbf{k}$ is the scattering vector, and $\mathbf{k}_\mathrm{p}$ is the wave vector having magnitude $\left|k_p\right| = 2\pi/\lambda''$. The energy transferred to the system in Compton process is

$$\Delta\omega = \hbar\omega_1 - \hbar\omega_2 = \left(k^2/2m_0\right) \quad \text{(A2)}$$

In terms of the Compton scattering angle $2\theta$,

$$k^2 = \left(k_1 - k_2\right)^2 = k_1^2 + k_2^2 - 2k_1k_2\cos 2\theta \quad \text{(A3)}$$

Typically, the energy of the X-ray photon is usually very high compared to its momentum. So, to a first approximation $\left|k_1\right|^2 \approx \left|k_2\right|^2$, so

$$k^2 = 2k_1^2 - 2k_1^2\cos 2\theta = 2k_1^2\left(1 - \cos 2\theta\right) \quad \text{(A4)}$$

Since, $\omega_1 = k_1c$ and $\omega_2 = k_2c$, the Eqn. (A2) may be written as

$$\Delta\omega = \left(\omega_1\omega_2/m_0c^2\right)\left(1 - \cos 2\theta\right) \quad \text{(A5)}$$

Simplifying Eqn. (A1) as per Eqn. (A2), similar to the case of electron in motion, gives

$$\Delta\omega\big|_N = \left(\omega_3 - \omega_1\right) + \left(k_p p_1/m_0\right)$$
$$\omega_3 = \Delta\omega\big|_N + \omega_1 - \left(k_p p_1/m_0\right) \quad \text{(A6)}$$

Again, modifying Eq. (A5) for this scattering, it gives

$$\Delta\omega\big|_N = \left(\omega_1\omega_3/m_0c^2\right)\left(1-\cos 2\theta'\right) \tag{A7}$$

Simple algebra using Eqn. (A6) and (A7) leads to the following result:

$$\omega_3 = \left(\omega_1\omega_3/m_0c^2\right)\left(1-\cos 2\theta'\right)+\omega_1-\left(k_p p_1/m_0\right) \tag{A8}$$

Finally, simplifying Eqn. (A8), energy of the scattered photon becomes

$$\omega_3 = \frac{\omega_1}{\left[1-\gamma\left(1-\cos 2\theta'\right)\right]} - \frac{\frac{1}{m}k_p p_1}{\left[1-\gamma\left(1-\cos 2\theta'\right)\right]} \tag{A9}$$

Simplifying the value of $k_p$, and applying the first approximation $|k_1|^2 \approx |k_3|^2$ as in Eqn. (A4), one can have

$$\begin{aligned} k_p &= \sqrt{(k_3-k_1)^2} = \sqrt{k_3^2+k_1^2-2k_1k_3\cos 2\theta'} \\ &= \sqrt{2k_1^2\left(1-\cos 2\theta'\right)} = 2\left(\frac{\omega_1}{c}\right)\sqrt{\sin^2\theta'} \end{aligned} \tag{A10}$$

Hence, the term $\frac{\hbar}{m_0}k_p p_1$ in Eqn. (A9), which is actually $\frac{1}{m_0}k_p p_1'$ and can be simplified to

$$\frac{1}{m_0}k_p p_1' = \frac{}{m_0}\left(2\left(\frac{\omega_1}{c}\right)\sqrt{\sin^2\theta'}\right).m_0v' = 2\,\omega_1\left(\frac{v'}{c}\right)\sqrt{\sin^2\theta'} \tag{A11}$$

## APPENDIX-B

Applying statistical model of the atom, the incoherent scattering cross section of X-rays by a system of interacting particles is expressible in terms of density distribution functions for the system [a, b] as follows:

$$\sigma(\mathbf{k}) = \sigma_T \int P(\mathbf{k},\mathbf{r})\, n(\mathbf{r})\, d\mathbf{r} \tag{B1}$$

where, $P(\mathbf{k},\mathbf{r})$ is the local correlation function, and $n(\mathbf{r})$ is the electron density function.

However, the maximum information about the many-particle system is contained in the quantity $P(\mathbf{k},\omega)$, which is the Fourier transformation in space and time of the time-dependent pair-distribution function for the system [a-d] or known as spectral function. The spectral function $P(\mathbf{k},\omega)$ is directly measured in an inelastic-scattering experiment. Applying the Born approximation, the angular and energy distribution of scattered photon defined as

$$\frac{d^2\sigma}{d\Omega\, d\omega} = \frac{{m_0}^2}{8\pi^3}\frac{p_3}{p_2} V_k^2\ P(\mathbf{k},\omega) \tag{B2}$$

for the particle (electron) of mass $m_0$, initial momentum $p_2$ scattered to a final momentum $p_3$, with energy transfer between $\omega$ and $\omega + d\omega$, and scattering angle specified by $d\Omega$.

In the case of collective mode, the Coulomb interaction factor [c], is simplified as

$$V_k = 4\pi\, e^2 / {k_p}^2 \tag{B3}$$

However, the static Coulomb interaction generated due to the scalar field (static field) [e], $\phi(\mathbf{r},t)$, a well-defined function of the particle coordinates at the same time.

Again, this $P(\mathbf{k},\omega)$ is related to the structure factor [c] $P(\mathbf{k})$ by

$$\int_{-\infty}^{\infty} P(\mathbf{k},\omega)\, d\omega = P(\mathbf{k})\, n_e \tag{B4}$$

where, $P(\mathbf{k}) = \left\langle \psi_o \left| \rho_k^{\dagger} \rho_k \right| \psi_o \right\rangle / n_e$, and the $P(\mathbf{k})$ is directly measured in a scattering experiment in which one determines the differential cross section. Then the differential cross section is determined by integrating over all energy transfer [c]:

$$\frac{d\sigma}{d\theta'} = \int_0^{\infty} \frac{d^2\sigma}{d\theta\, d\omega}\, d\omega = \frac{{m_0}^2}{8\pi^3}\frac{p_3}{p_1} V_k^2\ P(\mathbf{k})\, n_e \tag{B5}$$

Considering the interacting Fermi gas model (*i.e.*, the electrostatic interaction between electrons) which deals with relation between the pair distribution function and the dielectric constant of the uniform gas [b, f]. In the interacting Fermi gas model, the correlation term $P(\mathbf{k},\mathbf{r})$ used in the above Eqn. (B1) can be taken as $P(\mathbf{k})$ (for brevity by omitting the argument ($\mathbf{r}$) and can be expressed in the RPA as a function of dielectric constant $\in(\mathbf{k},\omega)$ as

$$P(\mathbf{k}) = \frac{k_p{}^2}{4\pi^2\, n_e\, e^2} \int_0^\infty \frac{\in_2(\mathbf{k},\omega)}{\left|\in(\mathbf{k},\omega)\right|^2}\, d\omega \tag{B6}$$

where, $\in(\mathbf{k},\omega) = \in_1(\mathbf{k},\omega) + i \in_2(\mathbf{k},\omega)$.

After a bit of algebraic simplification, one can have the $P(\mathbf{k})$ as the same as given in earlier Eqn. (B4). A quantized plasmon oscillation correspond to oscillations in the particle density. The collective contribution to $P(\mathbf{k})$ in the small $k_p$ region is, to an accuracy $k_p{}^4 / k_{TF}^4$,

$$P_{coll}(\mathbf{k}) = \frac{k_p{}^2}{2m\,\omega_k} \tag{B7}$$

where $\omega_k$ is the oscillation frequency of the collective mode with the wave number $k_p$ and $k_{TF}$ is the Thomas-Fermi screening wave number, $k_{TF}^2 = (4/\pi)(k_F / a_0)$, and $a_0$ is the Bohr radius [c].

The dielectric function $\varepsilon(\omega,k)$ of the electron gas, is strongly depends on the frequency and wavevector. The RPA is more also called the Lindhard dielectric function and is a model for a static $\varepsilon(k)$ or dynamic $\varepsilon(\omega,k)$ dielectric function [d]. For brevity, we do not exhibit here the frequency dependence (the predicted scattering is highly dependent on critical number density of plasom, $n_c$).

According to the dispersion relation, the collective frequency $\omega_k$ of the electromagnetic wave propagated in solid [g] can be simplified as

$$\omega_k = \left[\frac{c^2 k_p{}^2}{\varepsilon(\omega,k)}\right]^{\frac{1}{2}} = \left[\frac{4\pi\, c^2 k_p{}^2}{\in}\right]^{\frac{1}{2}} \tag{B8}$$

where, $\varepsilon = \varepsilon_0 \in$, and $\varepsilon_0 = 1/4\pi$

$$\omega_k = \left[\frac{c^2 k_p{}^2}{(n_c - n_e)/n_c}\right]^{\frac{1}{2}} \tag{B9}$$

Hence, simplifying Eqn. (B5) using expressions (B3), and (B7), one can have

$$\frac{d\sigma}{d\theta'} = \frac{{m_0}^2}{8\pi^3}\frac{p_3}{p_2}\left(\frac{4\pi\, e^2}{{k_p}^2}\right)^2 \frac{{k_p}^2}{2m_0\ \omega_k}\, n_e$$

$$= \frac{{m_0}^2}{8\pi^3}\frac{p_3}{p_2}\left(\frac{4\pi\, e^2}{{k_p}^2}\right)^2 \frac{{k_p}^2}{2m_0}\left[\frac{\in}{4\pi\, c^2 {k_p}^2}\right]^{\frac{1}{2}} n_e \quad \text{[substituting } \omega_k \text{ from (B8)}$$

$$= \left(\frac{e^2}{m_0 c^2}\right)^2\left(\frac{1}{k_p}\right)^3 \frac{(m_0 c)^4}{16\pi^3}\frac{p_3}{p_2}\frac{\hbar^2}{(m_0 c)}[4\pi]^{\frac{3}{2}}[\in]^{\frac{1}{2}} n_e \qquad \text{(B10)}$$

$$\text{Hence, } \frac{d\sigma}{d\theta'} = \sigma_T\left(\frac{1}{k_p}\right)^3 M_c\,\frac{p_3}{p_2}(\in)^{\frac{1}{2}} n_e \qquad \text{(B11)}$$

where $M_c$ ($\approx 2.756\times 10^4$) is a constant quantity, since, $m_0 c = 137$ and $\hbar = c = 1$. Since the solid angle $\Omega(\mathbf{r}, \theta')$ is a function of $\mathbf{r}$ and $\theta'$, the above Eqn. (B11) can be written as

$$\left(\frac{d\sigma}{d\Omega}\right)_N = \sigma_T\left(\frac{1}{k_p}\right)^3 M_c\,\frac{p_3}{p_2}(\in)^{\frac{1}{2}} n_e \qquad \text{(B12)}$$

[a]L.Von Hove, *Phys. Rev.*, **95**, (1954), 249.
[b]D. E. Parks and M. Rotenberg, *Phys. Rev.*, A**5**, (1972), 521.
[c]D. Pines, The Many-Body Problem, (Benjamin publications, New York, 1972).
[d]G. D. Mahan, Many-Particle Physics, (Kluwer Academic/ Plenum Publishers, New York, 2000).
[e]W. Heitler, Quantum Theory of Radiation, ed. N. F. Mott, E. C. Bullard and D. H. Wilkinson, (The University Press. Oxford, 1960) p.110 & 211.
[f]A. J. Glick, Lectures on the Many-Body Problem, ed. E. R. Caianiello, (Academic Press, New York, 1962).
[g]C. Kittel, Introduction to Solid State Physics, (Wily Eastern Ltd., New Delhi, 1994) p. 289.



*Peer-review history:*
*The peer review history for this paper can be accessed here:*
*http://www.sciencedomain.org/review-history.php?iid=283&id=4&aid=2239*